

## Challenges of an AC Line and a Parallel Mono-Polar DC Line Separated on a Same Right of Way

Ikbal Ali, Shahid Ahmad Dar, Sunil Kumar

Department of Electrical Engineering

Jamia Millia Islamia

New Delhi, India

<sup>1</sup>iali1@jmi.ac.in, <sup>2</sup>[shahid954110@gmail.com](mailto:shahid954110@gmail.com), skk7503@gmail.com

**Abstract: Ground resistivity, zero sequence currents, frequency response, phase domain modelling**

The purpose of this research is to look at the reason of significant zero sequence transients in ac lines caused by transients in a surrounding earth return dc circuit. A qualitative reasoning as well as a quantitative parametric examination are offered. The results reveal that even for relatively close lines, very significant transients can occur. Furthermore, transients appear only when non-zero ground resistivity is incorporated in the model. Different ground resistivities, earthing resistances, and the presence or absence of ground wires are also investigated. The document should be of interest to utilities that operate alternating current and direct current lines on the same right of way.

Keyword:

### I. Introduction:

Since nearly the beginning of electromagnetic transient simulation of power systems, transmission lines have been modelled in EMT type programs utilizing the modal analysis approach [7]. The earliest model used in EMT modelling was the classical Bergeron model, which estimated the capacitance and inductance of the line only at the fundamental frequency. However, the depth of current penetration into the ground and conductors is known to vary with frequency and resistivity. As a result, the capacitances and inductances of a transmission line are frequency dependent. This reality prompted the creation of frequency-dependent gearbox line models for use in EMT programs. The popular J. Marti modal-domain frequency dependent transmission line model introduced the first generation of these frequency-dependent models. Marti's frequency-dependent modal-domain transmission line model. Recently, phase domain frequency-dependent transmission line models [1–3] have been presented. For all frequencies, the modal-domain frequency-dependent transmission line models employ constant phase-to-mode and mode-to-phase transformation matrices. Only the depiction of the characteristic impedance and the attenuation of the different modes show the frequency dependence of the modal-domain models. This was a highly successful project. However, it is possible to demonstrate that the transformation matrices should likewise be frequency dependent. Unfortunately, when frequency dependent changes were added in EMT simulations, some of the simulations became numerically unstable. As a result, phase-domain frequency-dependent transmission line models were developed. To avoid difficulties with the frequency-dependence of the transformations, the phase-domain frequency-dependent transmission line models fully avoid employing phase-to-mode and mode-to-phase transformations. Bergeron line models are commonly employed in the modelling of alternating current systems. However, these models are incapable of accurately modelling the coupling of AC and DC lines on the same right-of-way [4].

The tripping of ac wires that shared a 240 kilometers path with two dc circuits inspired this study. Because of the operation of the ground current sensing relay, the ac lines tripped. The obvious source of the unexpected ground current

collection was the dc system's change from regular metallic return operation to ground return operation. Because of the huge zero sequence current detected in the ac line despite its distance (183 m) from the dc line, this phenomenon appeared extremely confusing. Because no induced current is observed during earth return steady state dc operation, it was determined to be a phenomenon linked with a dc line ground current transient. An inspection of the waveform, however, revealed that induction was present at very low frequencies but not at strict dc. As a result, it was decided to create a simplified model of the system that reflected all of the important aspects of the problem, such as ground resistivity effects [5] and various terminating impedances for the transformer neutrals. Using this model, a satisfactory explanation was discovered. The zero sequence pathways of the two (ac and dc) transmission circuits were modelled as two single conductor transmission lines for parametric research (Fig. 1). A current of 1 p.u. was injected (at various frequencies) into the 'dc' line, which was grounded at the other end. On either end of the 'ac' line, impedances to ground were installed. At line terminations, these represented the zero sequence impedances.

In order to analyze the induction effects as a function of frequency, the induced currents in the transmitting and receiving ends of the ac line were plotted as functions of frequency. The distance between the lines, ground resistivity, and contact resistance were all changed to see if they had any effect on the induced current.

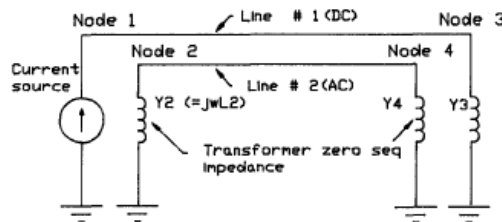


Figure 1. A simplified two conductor system with ground return

A ground wire was then installed above the ac line to check if it had any effect. The findings of this investigation reveal that the generated current is clearly caused by finite ground resistivity and does not appear when an infinitely conducting ground is considered. The induced currents are high (usually 20% of the zero-sequence current in the inducing line) and unaffected by the distance between the lines, grounding resistance, or the presence of a ground wire. The line itself is fairly detailed in its modelling. The parameters of the transmission line equations utilized are frequency dependent. Deri et al.1 (1) described a comparable approach.

## II. Problem Formulation

The transmission line equations for a U conductor transmission system are shown in Fig. 2. The voltage vector  $V$  denotes the phasor conductor voltages at every point  $x$  along the transmission line, that is,  $= [V_1, V_2, V_3, \dots, V_n]$  similarly, the vector current  $I$  reflects the phasor currents at  $x$ . In the equations,  $w$  is the frequency of the excitation voltage or current,  $Z(w)$  is the transmission line impedance (which varies with frequency  $w$ ), and  $Y(w)$  is the transmission line admittance.

$$\frac{d(V)}{dx} = Z(w)I \tag{1}$$

$$\frac{dI}{dx} = Y(w)V \tag{2}$$

$$z(w) = R(w) + j\omega L(w)$$

$$Y(w) = G(w) + j\omega C(w) \tag{3}$$

The self-impedance is represented by the diagonal entries  $Z_{ii}$  of the matrix  $Z$  and is approximated as (for two bundled conductors per line)

$$z_{ii} = z_{ii}(\text{int}) + z_{ii}(\text{ext}). \tag{4}$$

$$z_{ii}(\text{int}) = (\rho_i^m / 2\pi r_i \cot h(0.7777mr_i) + 0.3565\rho_i / \pi r_i^2) \Omega/\text{m} \tag{5}$$

$$\text{With } m = \sqrt[2]{\frac{j\omega\mu}{\rho_i}}$$

Eqn. 5 is a very high precision simplification of the more accurate expression utilizing Bessel Functions [3], according to Wedepohl & Wilcox (2). Deri & Semlyen [1] also provides an excellent approximation to Carson's [10] more exact expression for  $Z_{ii}(\text{ext})$ :

$$z_{ii}(\text{ext}) = \frac{j\omega\mu_0}{2\pi} \ln\left[\frac{2h_i + d_e}{r_i}\right] \tag{6}$$

Where  $d_e = \sqrt[2]{\frac{\rho}{j\omega\mu_0}}$  (the depth of penetration of the current flow below the ground).

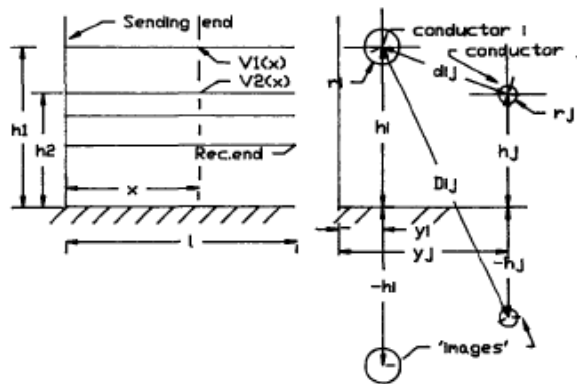


Figure 2: Model Geometry

$r_i$  = radius of conductor  $i$

$h_i$  = height above conductor of conductor  $i$

$\rho_i$  = resistivity of conductor  $i$

$P$  = ground resistivity

$\mu_0$  = permittivity free space

$$Z_{ij} = \frac{j\omega\mu_0}{2\pi} \ln\left(\sqrt{\frac{(y_i - y_j)^2 + (h_i + h_j + 2d_e)^2}{(y_i - y_j)^2 + (h_i - h_j)^2}}\right) \Omega/\text{m} \tag{7}$$

Similarly, for the frequencies of interest, namely those less than 100 kHz, the  $Y$  matrix in Eqn. 2 is derived as

$$Y = P^{-1} \quad \text{where } p = [p_{ij}] \quad i = 1 \dots n$$

$$J=1 \dots n \tag{8}$$

$$p_{ij} = 2\pi\omega\epsilon_o \int \ln \sqrt{(y_i - y_j)^2 + (h_i + h_j + 2de)^2} / d_{ij} \tag{9}$$

$$\text{Where } d_{ij} = \sqrt{(y_i - y_j)^2 + (h_i + h_j)^2} \quad \text{for } i \neq j$$

After obtaining the Y and Z matrices, equations 1 and 2 can be solved, and boundary conditions at the transmitting and receiving ends ( $V_o, I_o, V_l, I_l$  in Fig. 3) can be substituted to yield:

$$\begin{bmatrix} I_o \\ I_l \end{bmatrix} = \begin{bmatrix} Y_o & \coth(tl) & -Y_o \operatorname{cosec}(tl) \\ -Y_o & \operatorname{cosec}(tl) & Y_o \coth(tl) \end{bmatrix} \begin{bmatrix} V_o \\ V_l \end{bmatrix} \tag{10}$$

where  $I_o$  is a vector, whose components are the conductor currents at the sending end.  $V_o, I_l, V_l$  are vectors that are comparable. Here:

$$Y_o = Z^{-1}t \tag{11}$$

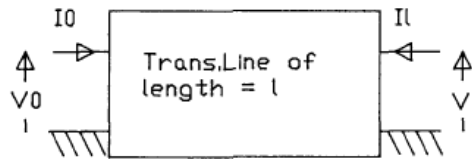


Figure 3. Two-port presentation

and is computed using conventional (eigenvalue-based) matrix function evaluation approaches (5)[11]. For the sake of a parametric research, it was decided to treat the two lines as single conductors (rather than a full three phase representation), as shown in Fig. 1. This keeps the situation simple enough to analyze the fundamental induction phenomena [8]. Furthermore, at a great distance (greater than the line's interphase intervals), the line seems to be a zero-sequence circuit with only one conductor. So, if two multiphase lines are separated by a significant distance, it is not too far off to view their zero sequence mutual effects as if they were a single conductor line. Equation (10) for the lines in figure. 1 for the sending end and receiving end can be rewritten as:

$$\begin{bmatrix} I_1 \\ I_2 \\ I_3 \\ I_4 \end{bmatrix} = \begin{bmatrix} Y_o \coth(tl) & Y_o \operatorname{cosec}(tl) \\ Y_o \operatorname{cosec}(tl) & Y_o \coth(tl) \end{bmatrix} \begin{bmatrix} V_1 \\ V_2 \\ V_3 \\ V_4 \end{bmatrix} \tag{12}$$

$I_1$  = injection line 1 sending end current

$$I_2 = -Y_2 V_2$$

$$I_3 = -Y_3 V_3 \tag{13}$$

$$I_4 = -Y_4 V_4$$

Equations (12) and (13) produce seven equations in the seven unknowns ( $I_1, I_2, I_3, I_4, V_1, V_2, V_3, V_4$ ), which are sufficient to solve for all of the unknowns.

### III. Parametric Studies:

- a) **Ignore Ground Resistivity:** fig.-4 depicts the induced current  $I_2$  assuming infinitely conducting ground ( $\rho=0 \Omega\text{-m}$ ) for a current injection  $I_1=1\text{A}$  for the two-conductor scenario represented in fig. 1 and data from Table I of the appendix. The frequency axis is in log (frequency), thus 0.00 corresponds to  $f=1 \text{ Hz}$ , 2.00 corresponds to  $f=100 \text{ Hz}$ , and so on. In the low frequency range ( $f<100 \text{ Hz}$  or  $\log f<2$ ), induced current is insignificant, in contrast to the considerable induction found in fig. 3. (A spectral study of Fig. 3's waveforms reveals that the frequencies of interest are in the 0-30 Hz range, with significant induced current evident at all of these frequencies.) The subsequent induced peaks at higher frequencies are caused by the influence of line capacitance, which is not as noticeable at lower frequencies. As a result, this graphic does not explain the induced current.

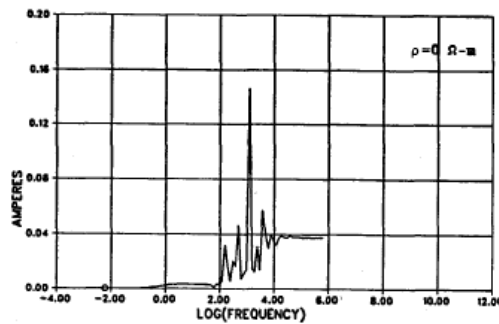


Fig 4. Frequency Response ( $I_2$ ) in the presence of a perfectly conducting earth

- b) **The Influence of Ground Resistance:** The current  $I_2$  (for  $I_1=1 \text{ p.u.}$  with variable frequency) for ground resistivities  $\rho$  of 10, 100, and 1000  $\Omega\text{-m}$  are shown in Fig. 5 a, b, and c, respectively. The induced current for  $\rho=10 \Omega\text{-m}$  is roughly 20% of the injected current  $I_1$  in the range  $f=10.56 \text{ Hz}$  ( $\log f = -0.25$ ) to  $f=30 \text{ Hz}$  ( $\log f=1.5$ ). Increasing  $\rho$  to 1000  $\Omega\text{-m}$  (fig. 5c) does not appear to have a commensurate effect on this induced current, which only climbs to 35% in the frequency range of interest. When comparing figures. 4 and 5a, it should be noticed that there is virtually no low frequency induction for  $\rho=0 \Omega\text{-m}$ , while there is considerable induction with a relatively low earth resistivity  $\rho=10 \Omega\text{-m}$ .  $I_2$  for  $\rho=100 \Omega\text{-m}$ , which is the average resistivity along the Nelson River Transmission line right of way, is shown in figure 5b. The time domain responses for an input waveform identical to the observed dc line current in fig. 3 for the  $\rho=100 \Omega\text{-m}$  example is shown in fig. 6. Take note of the similarity to the measured waveform in fig. 3. In comparison to the measured 1050 A in fig. 3, the maximal computed induced current is 925 A. It must be remembered that only a single conductor line representation was used. Also, an average ground resistivity of 100  $\Omega\text{-m}$  was used – a possible reason for this discrepancy. Also, the rate of decay is slower than observed. This may be attributed to a non-zero contact resistance as explained in a later section.

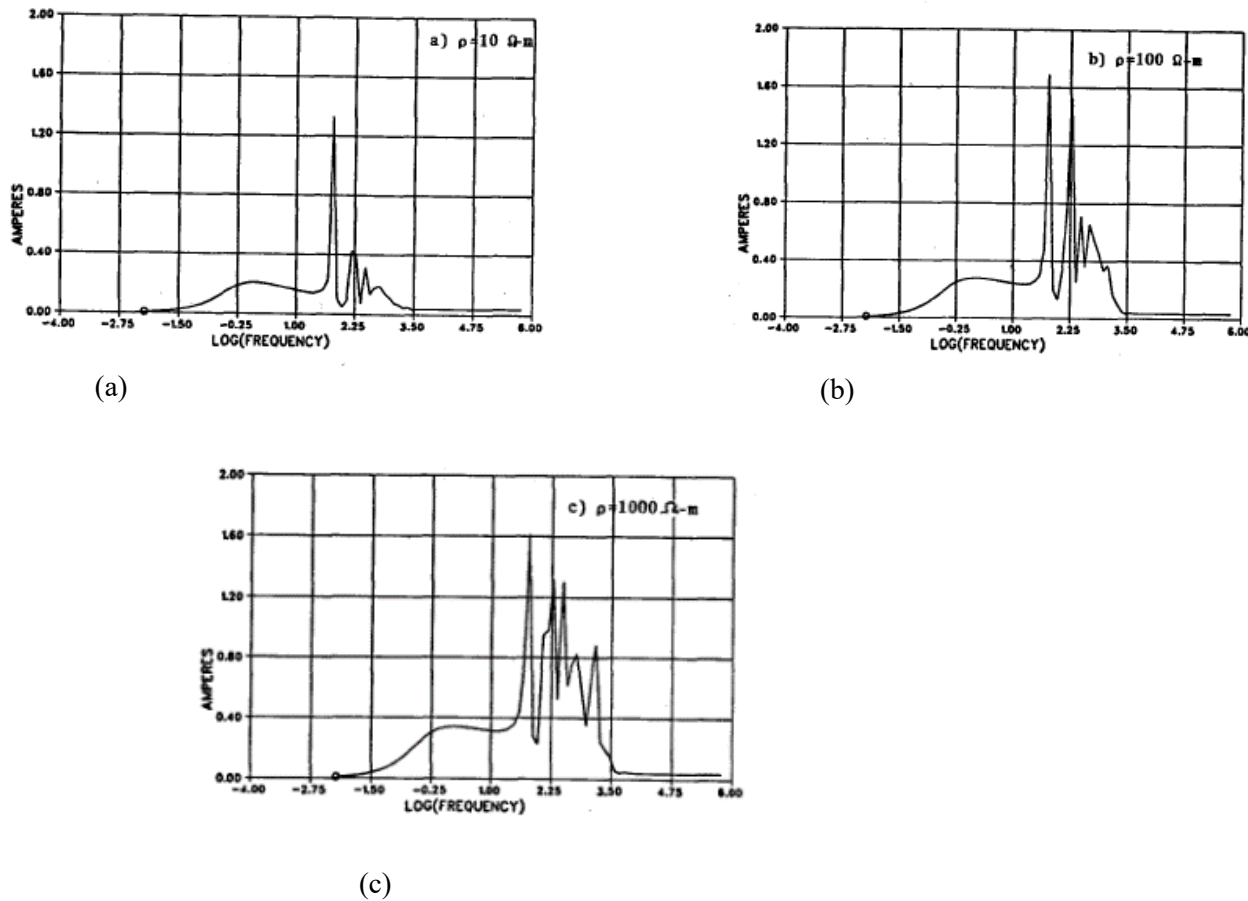


Figure. 5 The frequency response ( $I_2$ ) of the system when earth is considered a poor conductor.

- c) **The impact of changing the spacing between the lines:** Figures 7a and b illustrate the induced current for p-100  $\Omega$ -m for distances between the lines of 50m and 1000m, respectively. The same is seen in Fig. 5b for p-183 I, which is the average distance between GIA and the dc lines in the Manitoba Hydro System. The results reveal that even with a 1 km interline distance, the quantity of induction at low frequencies is relatively substantial (20%). As a result, the effect of dc line zero sequence transients can be felt in ac lines that are far away from the dc line. Higher frequency peaks, which are more a function of capacitive coupling, are projected to decrease as distance increases.
- d) **The Influence of Grounding Resistance:** In previous circumstances, it was thought that the transformer neutrals of the alternating current line had low impedance to ground. When compared to Fig. 8b, including a resistance in the zero-sequence path does not significantly reduce the induced current in the 1 Hz-30 Hz range, but it does tend to slightly reduce the induced current at the lowest frequencies, as shown in Fig. 8. (For example, compare the currents for  $\log(f)=-0.25$ . In Figs. 5b and 8, they are 0.24A and 0.18A, respectively). The temporal response for the same input current as in Fig. 6 for a grounding resistance of 2 $\Omega$  in the transformer neutral is shown in Fig. 9. When comparing Figs. 6 (for the zero-resistance scenario) and 9, it is clear that the peak generated currents are comparable, but the increased resistance causes the tail to decline faster. Fig. 9 appears to more nearly reflect the actual waveform (Fig. 3). The goal of this study is simply to show that the faster reported decay time may be a consequence of the grounding resistance, and that the value utilized in the prior solution (Fig. 6) may have been lower than the real resistance.

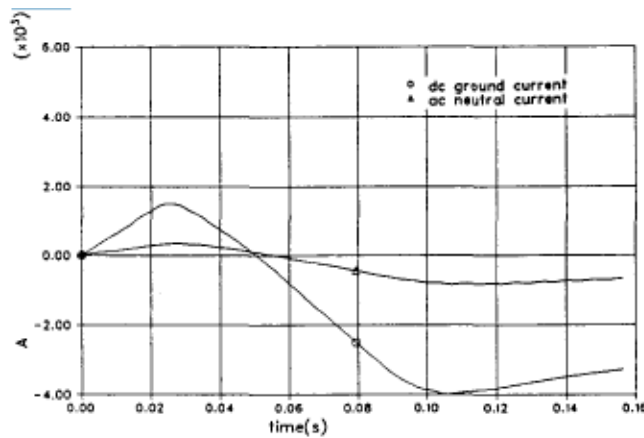


Figure 6: Simulated current waveform for the example shown in

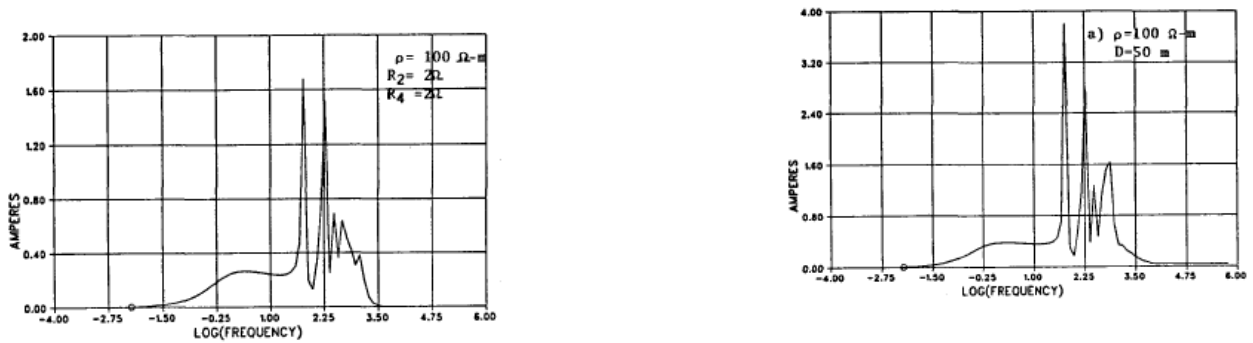


Fig 7. Frequency response ( $I_2$ ) at various interline lengths

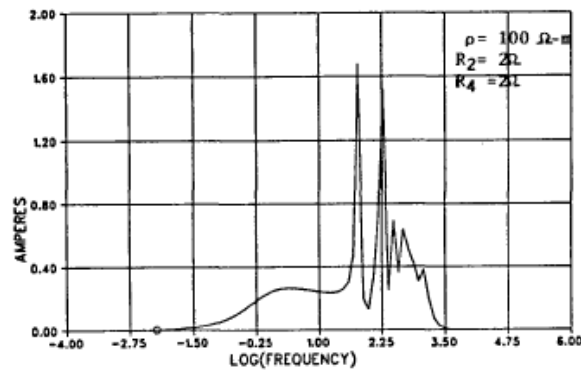


Fig 8. Frequency response ( $I_2$ ) with a  $2\Omega$  contact to ground on the neutrals of the sending and receiving end transformers.

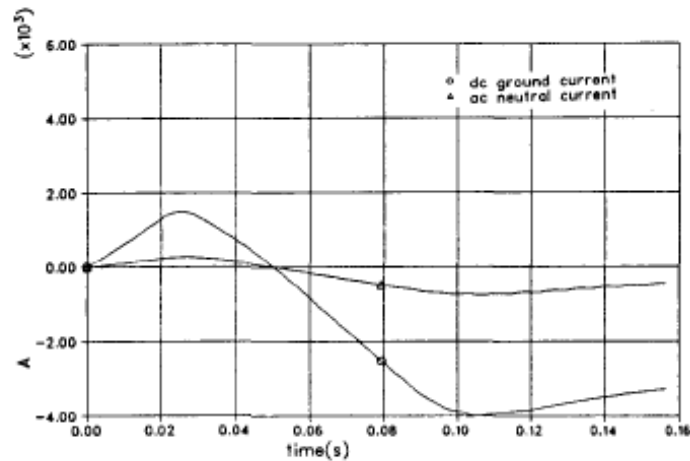


Fig.9. The effect of 'contact resistance to ground' on system response ( $I_2$ ).

The effect of a ground wire over an alternating current line: It was felt that a ground wire on the ac line would perhaps shield the line from this low frequency induction. The lines on which the phenomenon was observed did indeed have such a ground wire. To test this effect, a ground wire at a distance of 1 m above the conductor was incorporated in the model (data in Appendix). Fig. 10 shows the frequency response of the induced current (for  $\rho=100$  G-m), and comparison with Fig. 8b shows no appreciable effect at the lower frequencies.

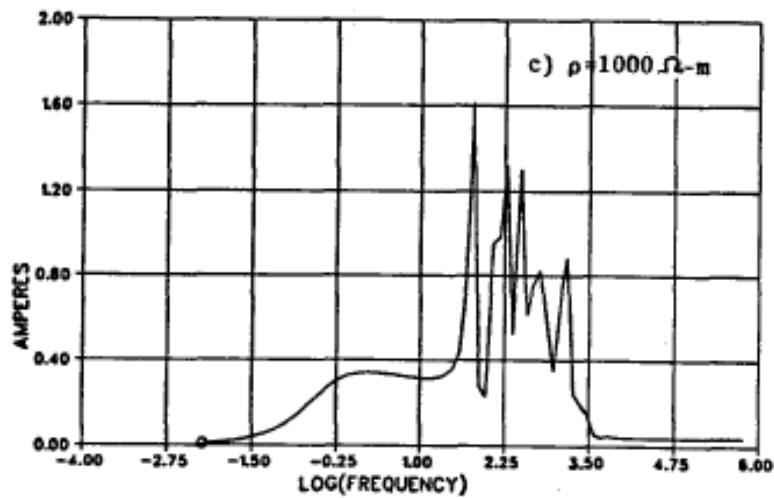


Figure 10. Frequency response ( $I_2$ ) in the presence of ground wire 2

IV. SIMULATION AND RESULTS:

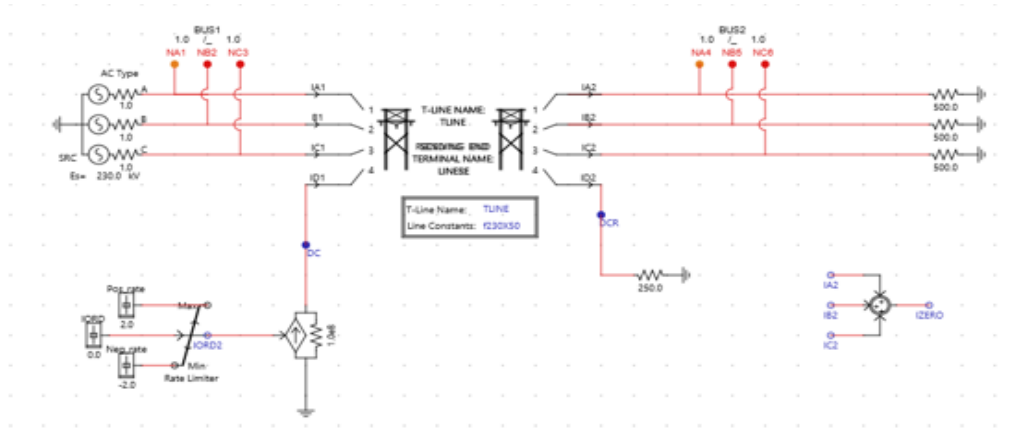
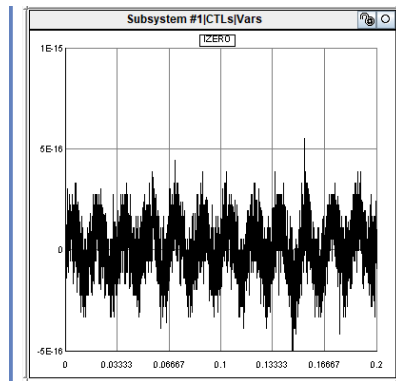
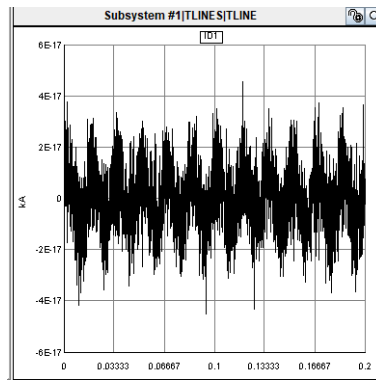


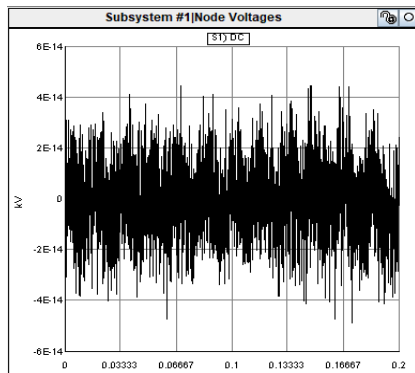
Figure 11. a 100km 230 kv AC line and a parallel mono-polar DC on a same right of way.



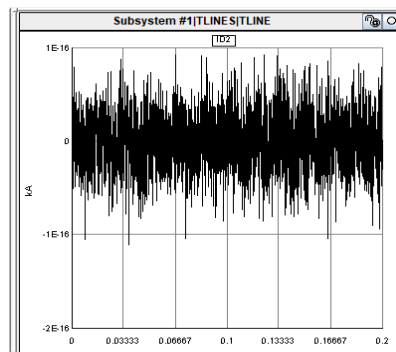
(a) zero-sequence currents



(b) DC current



(c) DC voltage



(d) ramped DC current

Figure 12. (a) zero-sequence currents (b) dc current (c) dc voltage (d) ramped dc current

At the moment, the phase-domain frequency dependent transmission line model in the RTDS Simulator can represent up to 12 parallel insulated conductors at a timestep of 50 microseconds.

In addition to the 12 insulated conductors, there are ground wires. On FPGA, a new tiny timestep frequency dependent transmission line model was recently developed. A transmission line with up to 12 linked conductors can be run at a timestep of 2.5- 3.0 microseconds using the small timestep concept. The graph a depicts the zero-sequence current in the AC line using the frequency-dependent phase-domain model. ID2 in graph d shows the ramping of the dc current which acts as a transient for our simulation model, When the ramping of DC current is finished and the di/dt of the DC line is zero, the zero-sequence current in the parallel AC line should also be zero. The parallel AC line's zero-sequence current should be transitory. Graph IZERO depicts a more accurate result for the zero-sequence current in the AC line provided by the frequency-dependent phase-domain transmission line model. Even with ground return, AC lines with grounded neutral transformers in the vicinity of a dc line do not experience any zero sequence currents during steady state operation of the dc circuit. Even the slowest transient in the dc circuit (with earth return operation) may create very significant zero sequence currents in the adjoining ac lines, perhaps triggering their protective mechanisms. This research aims to demonstrate the effect of altering the parameters associated with the two circuits on the induced current. Although the comparison of simulated and observed waveforms is not perfect, it is near enough to give confidence in using the relatively simplified (one conductor for each line) depiction. In any instance, rather than achieving a perfect match, the simplified model is utilized to highlight the sensitivity of the induced currents to the various factors. The following conclusions can be drawn.

#### V. Conclusion:

The phenomenon is unmistakably caused by non-zero ground resistivity. For  $p=0$ , no such low frequency induction is found. Significant induction is detected even at very low earth resistivity values ( $p=10\text{--}62\text{-m}$ ). This current is just moderately higher at the highest earth resistivities. At distances of up to 1 km between the lines, the induction impact can be significant. Ground wires atop the alternating current circuit do not effectively shield the alternating current circuits from these transients. Contact resistance to ground on transformer neutrals mostly suppresses very low frequencies. The initial transient peak is almost completely unaffected.

#### REFERENCES

- [1] R. Kuffel, R. P. Wierckx, H. Duchon, M. Lagerkvist, X. Wang, P. Forsyth, and P. Holmberg, "Expanding an analogue HVDC simulator's modelling capability using a real-time digital simulator (RTDS)," in First International Conference on Digital Power System Simulators – ICDS 95, College Station, Texas, U.S.A., 5–7 Apr., 1995, pp. 199–204.
- [2] RTDS Manual of Power System Components, RTDS Technologies Inc.
- [3] T. Maguire. (2011, Jun.). Multi-processor Cholesky decomposition of conductance matrices. Presented at International Conference on Power System Transients (IPST2011). [Online]. Available: [http://www.ipstconf.org/papers/Proc\\_IPST2011/11IPST106.pdf](http://www.ipstconf.org/papers/Proc_IPST2011/11IPST106.pdf)
- [4] N. Chopra, A. M. Gole, J. Chand, and R. W. Haywood, "Zero sequence currents in AC lines caused by transients in adjacent DC lines," IEEE Transactions on Power Delivery, vol. 3, no. 4, pp. 1873–1879, Oct. 1988.
- [5] Deri, A., Tevan, G., Semlyen, A., and Castanheira, A., "Homogeneous and Multi-Layer Earth Return", Trans. IEEE, Power Apparatus and Systems, 1981, pp. 3686-3693.
- [6] Wedepohl, L.M. and Uilcox, D.J., "Transient Analysis of Underground Power Transmission Systems", Proc. IEE, 1973, Vol. 120, No. 2, pp. 253-260.
- [7] R. Kuffel, T. Maguire, and Y. Zhang, "Recent developments in digital real time simulation for power systems," in Proceedings of WMSCI 2006, Orlando USA, July 2006, Paper No. S762HI.

- [8] B. Gustavsen, G. Irwin, R. Mangelrod, D. Brandt, and K. Kent, "Transmission line models for the simulation of interaction phenomena between parallel AC and DC overhead lines," in International Conference on Power System Transients (IPST1999), Budapest, Hungary, 20–24 Jul., 1999, pp. 61–67.
- [9] Shelkunoff, S.A., "The Electromagnetic Theory of CO-axial Transmission Lines and Cylindrical Shields", Bell System. Tech.J., 1934, Vol. 13,
- [10] Carson, J.B., "Wave Propagation in Overhead Wires, with Ground Return", Bell System. Tech.J., 1926, Vol. 5, pp. 539-554.
- [11] Wedepohl, L.M., 'Application of Matrix Methods to the Solution of Travelling Wave Phenomenon in Polyphase Systems', Proc. IEE, 1963, Vol. 110, pp. 532-579. NO. 12, pp. 2200-2212